Nano Energy 27 (2016) 275–281

Contents lists available at ScienceDirect

Nano Energy

journal homepage: www.elsevier.com/locate/nanoen

Biocompatibility and in vivo operation of implantable mesoporous PVDF-based nanogenerators

Yanhao Yu [a], Haiyan Sun [b], Hakan Orbay [c], Feng Chen [b], Christopher G. England [d], Weibo Cai [b,d], Xudong Wang [a,*]

[a] Department of Materials Science and Engineering, University of Wisconsin-Madison, Madison, WI 53706, USA
[b] Department of Radiology, University of Wisconsin-Madison, WI 53705, USA
[c] Department of Surgery, University of California-Davis, Sacramento, CA 95817, USA
[d] Department of Medical Physics, University of Wisconsin-Madison, Madison, WI 53705, USA

ARTICLE INFO

Article history:
Received 19 May 2016
Received in revised form
24 June 2016
Accepted 13 July 2016
Available online 16 July 2016

Keywords:
Biocompatibility
In vivo biomechanical energy harvesting
Mesoporous PVDF
Piezoelectric nanogenerator

ABSTRACT

The rapid developments of implantable biomedical electronics give rise to the motivation of exploring efficient and durable self-powered charging system. In this paper, we report a mesoporous polyvinylidene fluoride (PVDF)-based implantable piezoelectric nanogenerator (NG) for in vivo biomechanical energy harvesting. The NG was built with a sponge-like mesoporous PVDF film and encapsulated by polydimethylsiloxane (PDMS). After embedding this NG into rodents, a V_{oc} of ~200 mV was produced from the gentle movement of rodent muscle. Meanwhile, no toxicity or incompatibility sign was found in the host after carrying the packaged NG for 6 weeks. Moreover, the electric output of this NG was extremely stable and exhibited no deterioration after 5 days of in vivo operation or 1.512×10^8 times mechanical deformation. This NG device could practically output a constant voltage of 52 mV via a 1 μF capacitor under living circumstance. The outstanding efficiency, magnificent durability and exceptional biocompatibility promise this mesoporous PVDF-based NG in accomplishing self-powered bioelectronics with potentially lifespan operation period.

1. Introduction

Piezoelectric nanogenerator (NG) is a promising technology for harvesting mechanical energy from ambient environment relying on the electromechanical coupling effect of piezoelectric materials [1–4]. Due to the broad material selection and flexible structural design, NGs have shown superior capability in scavenging mechanical energy in various forms including acoustic waves, physical deflections, fluid or gas flows, and human activities [5–13]. Among them, in vivo biomechanical energy harvesting is particularly attractive since this approach could lead to a sustainable energy source for implantable biomedical devices, which could significantly reduce the volume of powering component and avoid battery replacement [14–16]. Considerable endeavors have been devoted in employing NGs to harvesting mechanical energy from the motion of muscle or organs like heart, lung and diaphragm [16–21]. Most NGs tested inside living organisms used piezoelectric ceramics, such as zinc oxide, [18,19] barium titanate, [22] and lead zirconate titanate (PZT) [17,21,23]. In order to achieve high flexibility, these materials were typically constructed in nanostructure and/or nanocomposite forms. On the other hand, piezoelectric polymers were directly used in NG design owing to their intrinsic superior flexibility and elasticity. β-phase polyvinylidene fluoride (PVDF) is the most widely used piezoelectric polymers with merits of high piezoelectric coefficients (20–30 pC/N for d_{33} and 16 pC/N for d_{31}), [24] excellent mechanical property and good biocompatibility [25–31]. These advantages encouraged a number of NG developments based on the piezoelectric PVDF [32–35].

Nevertheless, disregarding the great number of demonstrations of implantable NG designs, study of the biocompatibility and operation in a closed living biological environment is still very limited. The dynamic in vivo conditions could give rise to a number of critical issues that may not be a concern for in vitro tests. For example, the bio-fluid might respond to the polarized NG surfaces. Ions might infiltrate into the NG and deteriorate the piezoelectric property. The soft and irregular tissue surface might easily cause repelling or detachment of the NG component during normal body movement. It is also unclear how the biological surface would response to the high local piezoelectric potential generated in its vicinity. In this paper, we report a systematic study of the biocompatibility and in vivo operation of a mesoporous PVDF-based

* Corresponding author.
E-mail address: xudong.wang@wisc.edu (X. Wang).

http://dx.doi.org/10.1016/j.nanoen.2016.07.015
2211-2855/

flexible NGs. The NG was built with a sponge-like mesoporous PVDF film and encapsulated by polydimethylsiloxane (PDMS). The packaged NG was implanted under the skin of living mice and rats. Histological examination revealed no signs of toxicity or incompatibility during weeks of implantation. Appreciable piezoelectric output was obtained from the implanted NGs, which exhibited no deterioration after long-term in vivo operation. In vivo electricity routing and capacitor charging were also demonstrated inside the rat's body. This work provides valuable insights toward the biocompatibility and in vivo operation of flexible NGs for practically applications as an implantable biomechanical energy harvesting system.

2. Experimental section

2.1. Fabrication of Sponge-Like PVDF Thin Films

PVDF powder (Sigma Aldrich) was first dissolved in N,N-dimethylformamide (DMF) solvent with a concentration of 10 wt% at 70 °C. The PVDF solution was then mixed with ZnO nanoparticles (35–45 nm, US Research Nanomaterials, Inc.). The mass ratio between ZnO nanoparticles and PVDF was 50%. A uniformly distributed PVDF/ZnO suspension was obtained after treating the mixture in ultrasonic bath for 30 min. The suspension was then cast into a petri dish and dried in oven at 75 °C for approximate 10 min (depending on the film thickness). The films were subsequently immersed in a 37 wt% HCl solution for 3 h to completely remove the ZnO template. After acid etching and deionized water washing, the mesoporous PVDF thin films with a film thickness of ~30 μm were obtained.

2.2. Assembly and Measurement of PVDF NG

The mesoporous PVDF film was first cut to 1 cm × 2 cm and 100 nm-thick interdigitated surface gold electrode was deposited by electron beam evaporation with a shadow mask. Then, the PVDF film was poled using the interdigitated electrodes in an oil bath with an electric field of 60 V/μm for 2 h. After that, the PVDF film was sandwiched between two PDMS films with distinct film thicknesses (100 μm and 1 mm). The layered structure was then sealed by dipping and curing the liquid PDMS elastomer and cross-linker. During the performance measurement, a periodical deflecting force was applied on the NG device using a computer controlled shaker with a frequency of 20 Hz and a force of 6 N (quantified by a Force Gauge HF-500 N). The strain applied on the NG device was calculated to be ~0.1% on the basis of the cantilever model. The PDMS control sample was fabricated in a similar way by replacing the PVDF film with a PDMS film with identical film thickness. The voltage outputs were recorded using an Agilent DSO1012A oscilloscope. The current outputs were measured using an Autolab PGSTAT302N station. SEM image of mesoporous PVDF film was acquired with a LEO 1530 scanning electron microscope. FTIR characterizations of the PVDF films were performed by the Bruker Tensor 27 spectrometer.

2.3. Implantation of the PVDF NG

All animal studies were conducted under a protocol approved by the University of Wisconsin Institutional Animal Care and Use Committee. Adult Sprague-Dawley rats and six-week-old imprinting control region (ICR) mice (Harlan, Indianapolis, IN) were used to investigate the function of the NG in biological environment. Briefly, anesthesia was induced by inhalation of 2–5% isoflurane and maintained with 2% isoflurane. Following anesthesia, animals were fixed in the right lateral decubitus position. A 1–3 cm surgical incision was made to place the device. The NG was placed between the epithelial and muscle layer in the thigh or back region. The incision was sutured and the animal was connected to oscilloscope for measuring the voltage output. The NG was left under the skin and animals were allowed to recover. After the conclusion of studies, animals were euthanized and the NG, along with muscle, skin, and other tissues was collected for analysis. Computer tomography (CT) scans were performed using an Inveon microPET/microCT rodent model scanner (Siemens Medical Solutions USA, Inc.).

2.4. Biocompatibility safety assessment of NG in mice

In vivo toxicity was assessed in mice by surgically extracting the NG from the surgical site at select time points post-implantation. Tissue containing the muscle and skin, with the device between these two layers, was obtained for histological analysis. The NG was removed before tissues were paraffin embedded and sectioned at 5 μm thickness for analysis. For comparison, similar tissues were extracted from the contralateral leg, which contained no devices. Tissue sections were hematoxylin and eosin (H&E) stained before analysis. Toxicity of the tissue was assessed in sections using four criteria, including: (1) degree of inflammatory infiltrate; (2) degree of fibrosis; (3) presence of muscle degeneration; and (4) presence and degree of cellular toxicities at implantation device (e.g., cellular shrinkage, condensation of chromatin, cell membrane viability, and presence of apoptotic bodies).

3. Results and discussion

The mesoporous PVDF thin films were fabricated using ZnO nanoparticles (NPs) as the sacrificial template, following the approach we reported previously [34]. Removing the ZnO NPs left randomly distributed pores with sizes of 30–500 nm in the PVDF films (Fig. S1). The phase of the mesoporous PVDF films was characterized by the Fourier transform infrared (FTIR) spectrum (Fig. S2), where representative peaks of the piezoelectric β-phase at 840 and 1280 cm^{-1} could be clearly identified. The spontaneous formation of the β-phase was attributed to the interactions between the PVDF dipoles and surface charges on ZnO surfaces [7,34]. A fully assembled PVDF NG for implantation is shown in Fig. 1A. The mesoporous PVDF film was coated with a pair of interdigitated gold electrodes for piezoelectric charge collection, and the entire structure was packaged inside PDMS. According to our previous research, compared with the solid PVDF, introducing considerable porosity to the PVDF film could significantly increase its flexibility, [34] which is highly favorable for biomechanical energy harvesting. The interdigitated electrode was adopted to enable charge collection from the piezo vector of d_{33}, which has the highest piezoelectric coefficient for PVDF [24]. Meanwhile, the thicknesses of PDMS films that covered the top and bottom sides of the PVDF film were designed to be 100 μm and 1 mm, respectively. This variation of PDMS film thicknesses was able to increase the tension and compression portion of internal dipoles and thus improve device performance.

The energy harvesting capability of the completely-packaged NG was first characterized by periodically deflecting the NG in a cantilever mode. The open-circuit voltage (V_{oc}) and short-circuit current (I_{sc}) are presented in Fig. 1B and C, respectively. When the shaker was operating at 20 Hz with a force of 6 N and a strain of ~0.1%, the average values of V_{oc} and I_{sc} reached 3.8 V and 3.5 μA, respectively, which outperformed a number of reported PVDF-based NGs [6,30,32,33,36]. This superior performance was mostly attributed to the optimized device geometry and structural advantage of the mesoporous PVDF thin film. In comparison, after

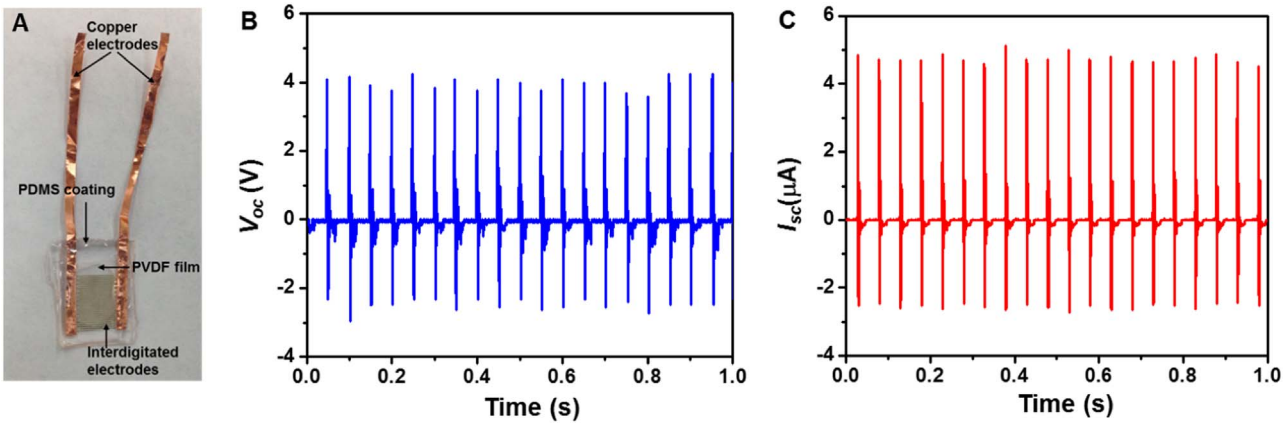

Fig. 1. In vitro electrical output of the PDMS-packaged PVDF NG. (A) A photograph of the PVDF NG before implantation. (B,C) The voltage (B) and current (C) output of the PVDF NG responding to a 20 Hz periodical deflection in a cantilever mode under in vitro condition.

replacing PVDF with PDMS (i.e., a representative triboelectric polymer with no piezoelectric response), the peak V_{oc} sharply reduced to ~0.1 V (Fig. S3), meaning the output of this NG design was predominately from the piezoelectric effects rather than triboelectric effects of the PVDF film. The high piezoelectric output also suggested that the PDMS packaging had minimal influence to the mechanical-to-electrical energy conversion.

To evaluate the biocompatibility, a PVDF NG with a size of 6 mm × 6 mm was inserted under the skin of mice's right leg (Fig. 2A and S4). The bottom layer of NG was attached to the quadriceps femoris muscle surface. Fig. 2B shows a CT scan of the mouse that carried the NG for 5 days, where the metal electrode could be clearly observed revealing the steady implantation position of the NG under the mouse's normal activity. The mice with implanted NG were sacrificed at week 1, 2, 3 and 6 for histological examination. Surgery and sham control groups were extracted from the right and left legs of the animal, respectively. As shown in Fig. 2C, surgical pathology analysis revealed no overall differences between the NG-implanted and sham thigh in terms of skin histology, as both sections appeared normal. There were limited inflammatory infiltrates in both groups. In addition, there were no signs of cellular toxicity or muscular atrophy/degeneration in tissue sections. As expected, the surgical thigh and sham thigh showed regional disruption in the epidermal layer, which was attributed to the formation of scar tissue and wound healing. Overall, there were no signs of toxicity or incompatibility induced

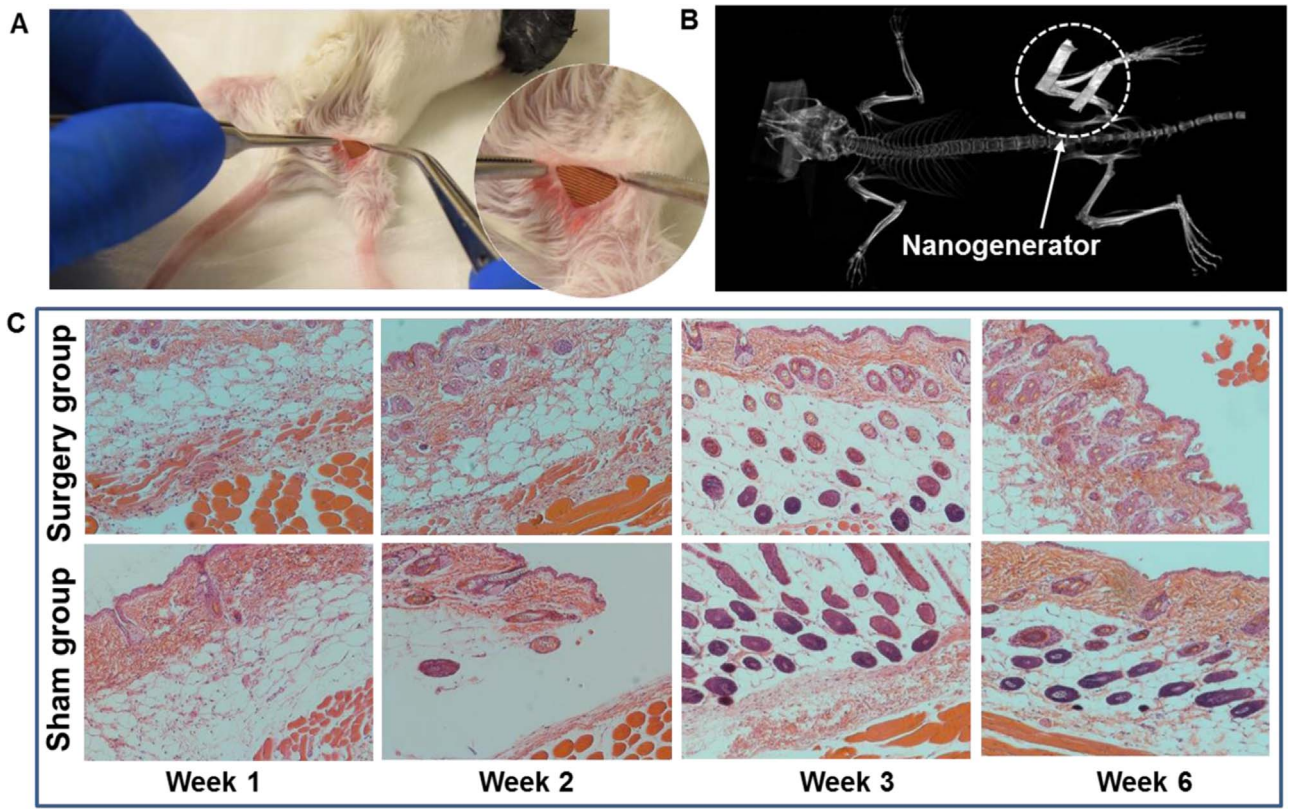

Fig. 2. Biocompatibility assessment of the PDMS-packaged PVDF NG. (A) A surgery picture of the mouse with the PVDF NG embedded between the epithelial and muscle layer in the thigh region. Inset is an enlarged picture showing the implanted PVDF NG with integrated surface electrode. (B) CT scan of a mouse that carried the NG for 5 days, revealing the steady implantation position of the NG under mouse's normal activity. (C) Surgical pathology analysis of the NG-implanted and sham group at week 1, 2, 3 and 6 after implantation. No signs of toxicity or incompatibility induced by the NG were observed in terms of muscle and skin histology.

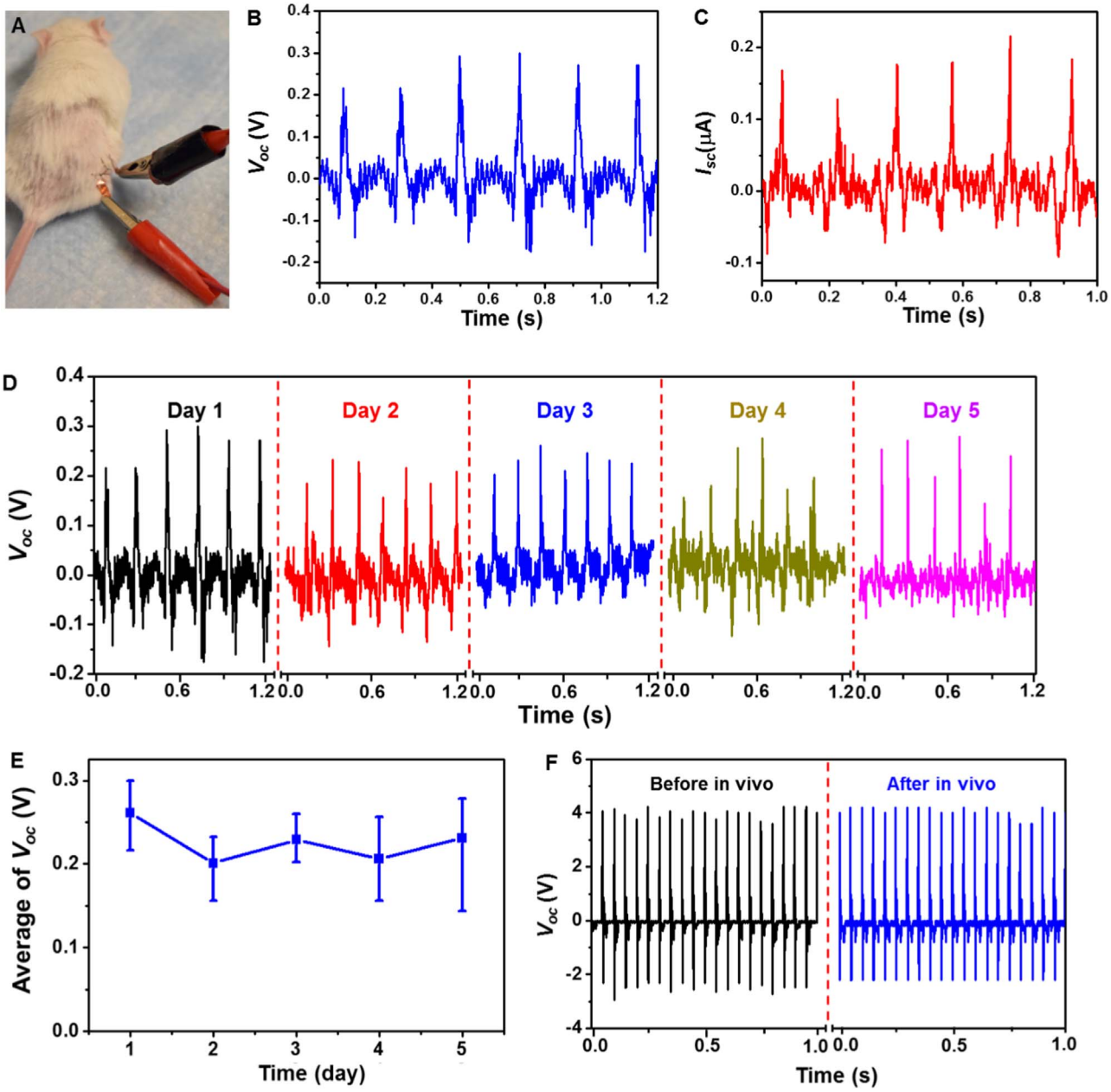

Fig. 3. In vivo electrical output of the PDMS-packaged PVDF NG. (A) A photograph of the connection setup during the in vivo measurement of the electricity generation. (B,C) In vivo voltage (B) and current (C) output of the PVDF NG upon movement of the rat's leg. (D) The voltage output of the PVDF NG within 5 days while the rats lived under normal conditions. (E) The variation of voltage output as a function of the testing period. The fairly stable signal indicates good durability of this NG device under normal activity of the rats. (F) Comparison of in vitro V_{oc} before and after 5 days of implantation.

by the NG in mice, suggesting excellent biocompatibility of the PDMS-packaged PVDF NG system.

The in vivo biomechanical energy harvesting experiments were then conducted in living rats. An NG with size of 1 cm × 2 cm was implanted between the epithelial and muscle layer in the thigh region of a rat through a 1–3 cm surgical incision (Fig. 3A). Subsequently, the incision was sutured with two electrode leads through the wound. During the measurement, the animal was under anesthesia and its leg with NG was manually deflected. Instantaneous voltage output was obtained upon the motion of the animal's leg, suggesting the quick response of the NG (see video S1). Fig. 3B and C shows the V_{oc} and I_{sc} characterizations of the NG under in vivo condition. The average values of V_{oc} and I_{sc} were found to be 0.26 V and 0.17 μA, respectively. Compared with the in vitro outputs, both V_{oc} and I_{sc} were greatly reduced due to the dramatically restricted deformation amplitude of the PVDF film in the biological environment. However, since the power outputs of the piezoelectric NG are directly proportional to the dimension and deformation scale of the device, significant performance enhancement could be expected when the NG is implanted inside larger body areas such as the human body.

Supplementary material related to this article can be found online at: http://dx.doi.org/10.1016/j.nanoen.2016.07.015.

After the initial implantation, the device was left inside the rats for 5 days to examine the long-term durability and performance in an in vivo environment. The V_{oc} was measured repeatedly every day while the rats were housed under normal conditions (Fig. 3D). The peak V_{oc} were determined to be 0.26 ± 0.03 V, 0.20 ± 0.03 V, 0.23 ± 0.02 V, 0.21 ± 0.04 V, 0.23 ± 0.05 V for day 1–5, respectively (Fig. 3E). The stable V_{oc} within the entire experimental period

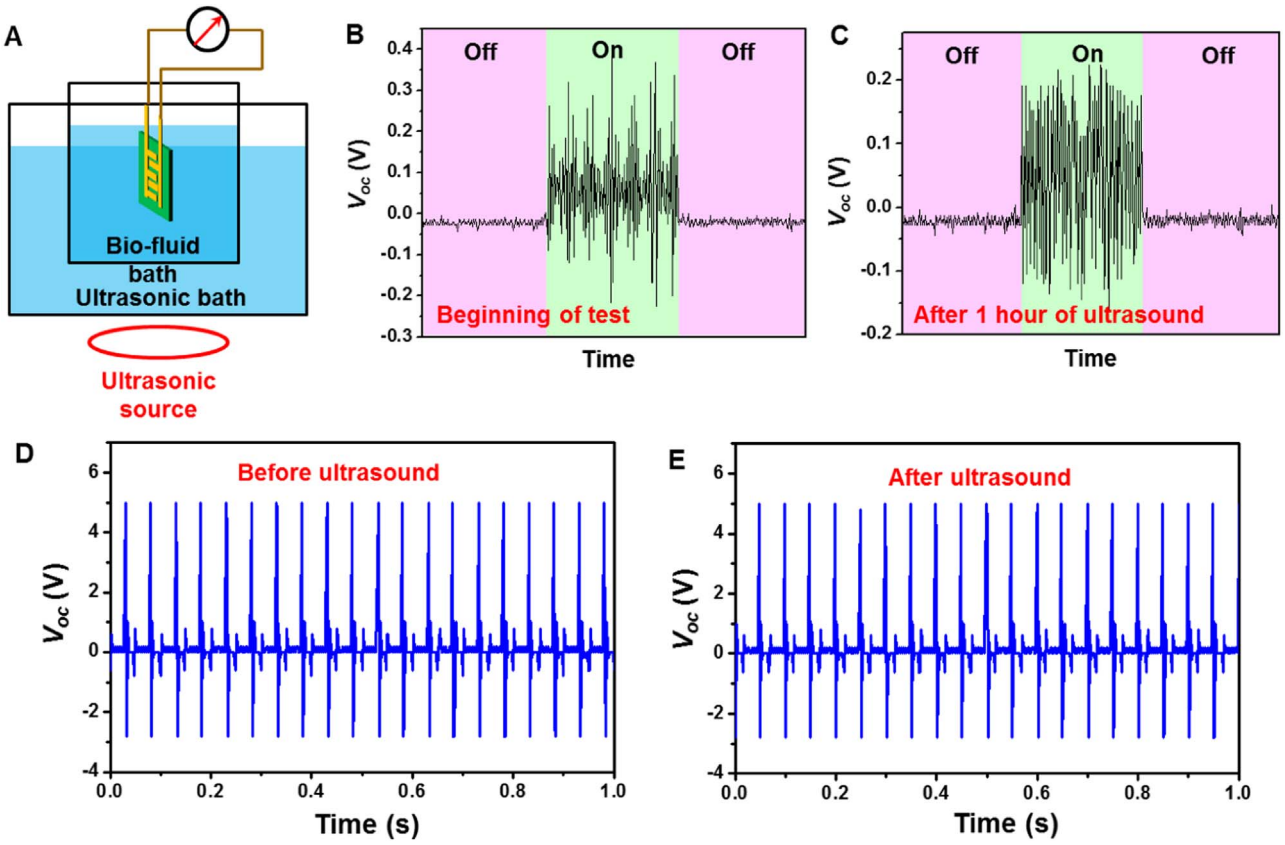

Fig. 4. Long-term durability evaluation of the PDMS-packaged PVDF NG. (A) Schematic illustration of the mimic bio-environment with ultrasonic wave as the vibration source. (B,C) The voltage output of the PVDF NG at the beginning (B) and after 1 h of ultrasound (C). On and off represent with and without ultrasonic vibration. (D,E) Comparison of in vitro V_{oc} before (D) and after (E) the ultrasound.

suggested that the NG device could function normally without noticeable decay, despite the constant motion of the animal during the five days. After 5 days of embedment, the PVDF NG was taken out from the rat's body and its piezoelectric output was re-characterized under the same in vitro deflection conditions. No obvious discrepancy was observed from the V_{oc} signals of NG before (black) and after (blue) 5 days of implantation in live rats (Fig. 3F). This comparison confirmed the well preserved functionality of the NG after experiencing long time exposure to the body fluid and tremendous/constant irregular mechanical deformation.

Nevertheless, the desired life time for an implantable NG should be at least multiple years in order to effectively minimize the chance of surgical replacement. Using heart beating as an example, given the typically beating frequency being 60 per minute, 5 years of operation requires $\sim 1.577 \times 10^8$ straining actions. In order to evaluate the possible life time of the packaged NG for converting heart motion to electricity within a reasonable time frame, ultrasonic wave was introduced as the vibration source to mimic the straining from heart beating over life time. As schematically shown in Fig. 4A, the entire NG device was immersed in the 0.9% NaCl solution and was subjected to continuous straining in an ultrasonic bath. The ultrasonic source was operating at a frequency of 42 kHz. By considering one strike by the acoustic wave as one straining action to the NG, one hour of ultrasound bath ideally corresponded to 1.512×10^8 straining actions, which was about the same as the number of heart beat in 5 years. It should be noted that this estimation was established without considering the variable displacement scales of ultrasonic wave and human heart beat. The voltage output was measured when the ultrasonic source was turned on and off. Clear voltage output was identified when turning on the ultrasonic equipment. The average peak value of V_{oc} was found to be $\sim 0.2 \pm 0.1$ V, which was comparable to that of in vivo measurement (Fig. 4B). This relatively small value was a consequence of the limited straining amplitude from ultrasonic wave. After 1 h of continuous operation, the NG was able to produce a more consistent V_{oc} of $\sim 0.18 \pm 0.03$ V (Fig. 4C). This comparison revealed that the PDMS packaging was highly robust and was able to protect the PVDF NG from bio-fluids under long-term mechanical deformation. The piezoelectric voltage outputs of the NG were further compared before and after the ultrasonic agitation outside of bio-fluids under a mechanical shaker. As shown in Fig. 4D and E, the V_{oc} curves were almost identical before and after the ultrasonic bath, confirming the piezoelectric performance of the packaged PVDF NG were not impaired by long-term straining actions in bio-fluids. This study demonstrated the excellent durability of the PDMS-packaged PVDF NG and endowed practical application potential of this NG system as an implantable power source of biomedical devices.

The efficient and stable electric output promised the PVDF NG in charging or powering small electronics in vivo. To demonstrate this point, an energy storage system comprised of a miniaturized bridge circuit and a ceramic capacitor (1 μF) was packaged (Fig. 5A). As shown in Fig. 5B and C, the NG was implanted following the same procedure as abovementioned implantation experiments. The output leads of the NG was wired through the epithelial and muscle layer in the thigh and back region, and extended out from the back of the rat where the motion is minimized. The energy storage pack was then connected through the leads and fixed on the back of the rat. Upon the movement of the rat's leg, the NG was straining and generating electricity as expected. After the rectification, the alternating current (AC) was

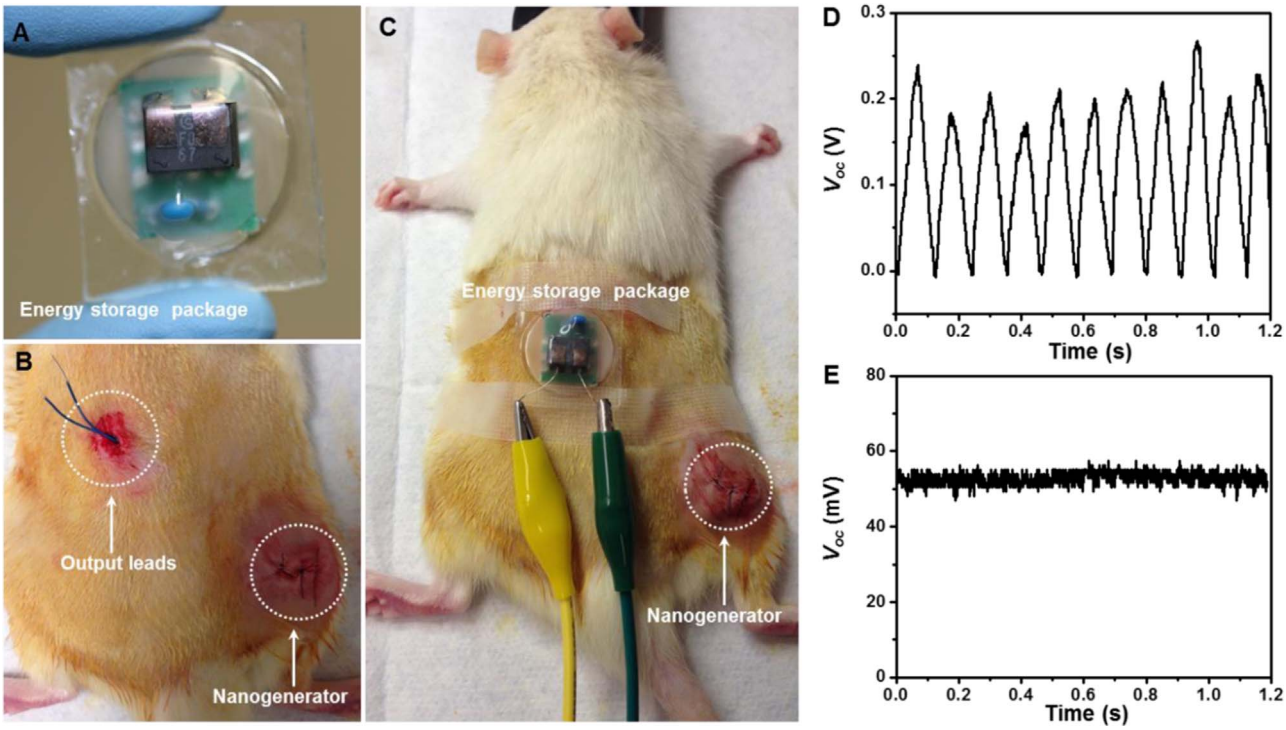

Fig. 5. Demonstration of practical biomechanical energy conversion and storage in live rats. (A) A photograph of the energy storage package composed of a miniaturized bridge circuit and a ceramic capacitor (1 μF). (B) A photograph of implanted PVDF NG in a rat with extended output leads. (C) Overall setup of the in vivo electricity generation and storage in rats. (D) DC voltage output from the PVDF NG after rectification. (E) Constant voltage output from NG charged energy storage package.

converted to direct current (DC) signal without observable loss through the in vivo electricity transport (Fig. 5D). The peak value of V_{oc} after rectification reached about 200 mV, which was similar as the AC signal. This output was converted to a 52 mV DC voltage through a 1 μF capacitor (Fig. 5E), suggesting good potential of using NG to power biomedical electronics in vivo.

4. Conclusion

In summary, we developed an efficient, flexible and robust piezoelectric polymer-based NG system with the capability of harvesting biomechanical energy in living organism. The size, structure and packaging of the NG were designed delicately for adapting the harsh in vivo environment. Due to the optimized device configuration and excellent flexibility of the sponge-like mesoporous PVDF film, the average V_{oc} and I_{sc} of this NG device reached 3.8 V and 3.5 μA, respectively, outperforming a number of reported PVDF-based NGs. By implanting the packaged NG to the quadriceps femoris muscle surface of a rat, a V_{oc} of ~200 mV was generated from the gentle motions of the rat's leg; and this signal exhibited no reduction after 5 days of in vivo operation. Years-long operation of the packaged NG in biological environment was predicted by testing the NG in ultrasonic bio-fluid bath. The electricity produced from animal's leg movement was transported in vivo by buried leads and connected to an energy storage pack located remotely. The generated AC signals were rectified and a DC output of ~52 mV was obtained through a capacitor. This study demonstrated that packaged PVDF NG could be a feasible strategy to serve as implantable powering system with practically long life time.

Acknowledgments

Research reported in this publication was supported, in part, by the National Institutes of Health (R01EB021336, R01CA169365, P30CA014520, and T32CA009206). The content is solely the responsibility of the authors and does not necessarily represent the official views of the National Institutes of Health.

Appendix A. Supporting information

Supplementary data associated with this article can be found in the online version at http://dx.doi.org/10.1016/j.nanoen.2016.07.015.

References

[1] Z.L. Wang, J. Song, Science 312 (2006) 242–246.
[2] X. Wang, J. Song, J. Liu, Z.L. Wang, Science 316 (2007) 102–105.
[3] X. Wang, Nano Energy 1 (2012) 13–24.
[4] Y. Hu, Z.L. Wang, Nano Energy 14 (2015) 3–14.
[5] S.N. Cha, J.S. Seo, S.M. Kim, H.J. Kim, Y.J. Park, S.W. Kim, J.M. Kim, Adv. Mater. 22 (2010) 4726–4730.
[6] B.J. Hansen, Y. Liu, R. Yang, Z.L. Wang, ACS Nano 4 (2010) 3647–3652.
[7] M. Lee, C.Y. Chen, S. Wang, S.N. Cha, Y.J. Park, J.M. Kim, L.J. Chou, Z.L. Wang, Adv. Mater. 24 (2012) 1759–1764.
[8] K.I. Park, M. Lee, Y. Liu, S. Moon, G.T. Hwang, G. Zhu, J.E. Kim, S.O. Kim, D. K. Kim, Z.L. Wang, K.J. Lee, Adv. Mater. 24 (2012) 2999–3004.
[9] J.-H. Lee, K.Y. Lee, B. Kumar, N.T. Tien, N.-E. Lee, S.-W. Kim, Energy Environ. Sci. 6 (2013) 169–175.
[10] S. Siddiqui, D.-I. Kim, L.T. Duy, M.T. Nguyen, S. Muhammad, W.-S. Yoon, N.-E. Lee, Nano Energy 15 (2015) 177–185.
[11] Y. Yu, Z. Li, Y. Wang, S. Gong, X. Wang, Adv. Mater. 27 (2015) 4938–4944.
[12] M. Zhang, T. Gao, J. Wang, J. Liao, Y. Qiu, Q. Yang, H. Xue, Z. Shi, Y. Zhao, Z. Xiong, L. Chen, Nano Energy 13 (2015) 298–305.
[13] Y. Yu, X. Wang, Extreme Mech. Lett. (2016), http://dx.doi.org/10.1016/j.eml.2016.02.019.

[14] Q. Zheng, B. Shi, F. Fan, X. Wang, L. Yan, W. Yuan, S. Wang, H. Liu, Z. Li, Z. L. Wang, Adv. Mater. 26 (2014) 5851–5856.
[15] G.T. Hwang, D. Im, S.E. Lee, J. Lee, M. Koo, S.Y. Park, S. Kim, K. Yang, S.J. Kim, K. Lee, K.J. Lee, ACS Nano 7 (2013) 4545–4553.
[16] G.T. Hwang, Y. Kim, J.-H. Lee, S. Oh, C.K. Jeong, D.Y. Park, J. Ryu, H.S. Kwon, S.-G. Lee, B. Joung, D. Kim, K.J. Lee, Energy Environ. Sci. 8 (2015) 2677–2684.
[17] S.R. Platt, S. Farritor, K. Garvin, H. Haider, IEEE/ASME Trans. Mechatron. 10 (2005) 455–461.
[18] R. Yang, Y. Qin, C. Li, G. Zhu, Z.L. Wang, Nano Lett. 9 (2009) 1201–1205.
[19] Z. Li, G. Zhu, R. Yang, A.C. Wang, Z.L. Wang, Adv. Mater. 22 (2010) 2534–2537.
[20] A. Zurbuchen, A. Pfenniger, A. Stahel, C.T. Stoeck, S. Vandenberghe, V.M. Koch, R. Vogel, Ann. Biomed. Eng. 41 (2013) 131–141.
[21] C. Dagdeviren, B.D. Yang, Y. Su, P.L. Tran, P. Joe, E. Anderson, J. Xia, V. Doraiswamy, B. Dehdashti, X. Feng, B. Lu, R. Poston, Z. Khalpey, R. Ghaffari, Y. Huang, M.J. Slepian, J.A. Rogers, Proc. Natl. Acad. Sci. 111 (2014) 1927–1932.
[22] K.I. Park, S. Xu, Y. Liu, G.T. Hwang, S.J. Kang, Z.L. Wang, K.J. Lee, Nano Lett. 10 (2010) 4939–4943.
[23] Y. Qi, J. Kim, T.D. Nguyen, B. Lisko, P.K. Purohit, M.C. McAlpine, Nano Lett. 11 (2011) 1331–1336.
[24] P. Ueberschlag, Sens. Rev. 21 (2001) 118–126.
[25] R.A. Whiter, V. Narayan, S. Kar-Narayan, Adv. Energy Mater. 4 (2014) 1400519.
[26] B.S. Lee, B. Park, H.S. Yang, J.W. Han, C. Choong, J. Bae, K. Lee, W.R. Yu, U. Jeong, U.I. Chung, J.J. Park, O. Kim, ACS Appl. Mater. Interfaces 6 (2014) 3520–3527.
[27] S. Garain, T.K. Sinha, P. Adhikary, K. Henkel, S. Sen, S. Ram, C. Sinha, D. Schmeisser, D. Mandal, ACS Appl. Mater. Interfaces 7 (2015) 1298–1307.
[28] N.R. Alluri, B. Saravanakumar, S.J. Kim, ACS Appl. Mater. Interfaces 7 (2015) 9831–9840.
[29] X. Chen, H. Tian, X. Li, J. Shao, Y. Ding, N. An, Y. Zhou, Nanoscale 7 (2015) 11536–11544.
[30] J.-H. Lee, H.-J. Yoon, T.Y. Kim, M.K. Gupta, J.H. Lee, W. Seung, H. Ryu, S.-W. Kim, Adv. Funct. Mater. 25 (2015) 3203–3209.
[31] C. Chang, V.H. Tran, J. Wang, Y.K. Fuh, L. Lin, Nano Lett. 10 (2010) 726–731.
[32] S.H. Bae, O. Kahya, B.K. Sharma, J. Kwon, H.J. Cho, B. Ozyilmaz, J.H. Ahn, ACS Nano 7 (2013) 3130–3138.
[33] M. Baniasadi, J. Huang, Z. Xu, S. Moreno, X. Yang, J. Chang, M.A. Quevedo-Lopez, M. Naraghi, M. Minary-Jolandan, ACS Appl. Mater. Interfaces 7 (2015) 5358–5366.
[34] Y. Mao, P. Zhao, G. McConohy, H. Yang, Y. Tong, X. Wang, Adv. Energy Mater. 4 (2014) 130624.
[35] C. Sun, J. Shi, D.J. Bayerl, X. Wang, Energy Environ. Sci. 4 (2011) 4508.
[36] J.H. Lee, K.Y. Lee, M.K. Gupta, T.Y. Kim, D.Y. Lee, J. Oh, C. Ryu, W.J. Yoo, C.Y. Kang, S.J. Yoon, J.B. Yoo, S.W. Kim, Adv. Mater. 26 (2014) 765–769.